The Virgo 3 km interferometer for gravitational wave detection

F. Acernese, P. Amico, M. Alshourbagy, F. Antonucci, S. Aoudia, P. Astone, S. Avino, L. Baggio, G. Ballardin, F. Barone, et al.

THE VIRGO 3-KM INTERFEROMETER FOR GRAVITATIONAL WAVE DETECTION

F.Acernese[5], P.Amico[9], M. Alshourbagy[10], F. Antonucci[11], S.Aoudia[6], P. Astone[11], S. Avino[5], G.Ballardin[2], F.Barone[5], L.Barsotti[10], M.Barsuglia[7], Th. S. Bauer[12], F.Beauville[1], S. Bigotta[10], M.A.Bizouard[7], C.Boccara[8], F.Bondu[6], L.Bosi[9], C.Bradaschia[10], J. F. J. van den Brand[12], S. Birindelli[10], S.Braccini[10], A.Brillet[6], V.Brisson[7], D.Buskulic[1], E.Calloni[5], E.Campagna[3], F. Carbognani[2], F.Cavalier[7], R.Cavalieri[2], G.Cella[10], E.Cesarini[3], E.Chassande-Mottin[6], A.-C.Clapson[7], F.Cleva[6], E. Coccia[13], C. Corda[10], A. Corsi[11], F.Cottone[9], J.-P.Coulon[6], E.Cuoco[2], S. D'Antonio[13], A. Dari[9], V.Dattilo[2], M.Davier[7], M. del Prete[10], R.De Rosa[5], L.Di Fiore[5], A.Di Virgilio[10], B.Dujardin[6], A.Eleuteri[5], M. Evans[2], V. Fafone[13], I.Ferrante[10], F.Fidecaro[10], I.Fiori[2], R.Flaminio[1,2], J.-D.Fournier[6], S.Frasca[11], F.Frasconi[10], L.Gammaitoni[9], F.Garufi[5], E.Genin[2]*, A.Gennai[10], A.Giazotto[10], L. Giordano[5], R. Gouaty[1], V. Granata[1], D. Grosjean[1], G.Guidi[3], S. Hamdani[2], S.Hebri[2], H.Heitmann[6], P.Hello[7], D. Huet[2], S. Karkar[1], S.Kreckelbergh[7], P.La Penna[2], M. Laval[6], N. Leroy[7], N.Letendre[1], B. Lopez[2], M. Lorenzini[3], V.Loriette[8], G.Losurdo[3], J.-M.Mackowski[4], E.Majorana[11], C.N.Man[6], M. Mantovani[10], F. Marchesoni[9], F.Marion[1], J. Marque[2], F.Martelli[3], A.Masserot[1], F. Menzinger[2], L.Milano[5], Y. Minenkov[13], C. Moins[2], J.Moreau[8], N.Morgado[4], B.Mours[1], I.Neri[9], F. Nocera[2], G. Pagliaroli[13], G.V. Pallottino[11], C.Palomba[11], F.Paoletti[2;10], S. Pardi[5], A. Pasqualetti[2], R. Passaquieti[10], D. Passuello[10], F. Piergiovanni[3], L.Pinard[4], R.Poggiani[10], M.Punturo[9], P.Puppo[11], S. van der Putten[12], K.Qipiani[5], P.Rapagnani[11], V.Reita[8], A.Remillieux[4], F.Ricci[11], I.Ricciardi[5], A. Rocchi[13], P. Ruggi[2], G.Russo[5], S.Solimeno[5], A. Spallicci[6], M. Tarallo[10], R. Terenzi[13], M. Tonelli[10], A. Toncelli[10], E.Tournefier[1], F.Travasso[9], C. Tremola[10], G. Vajente[10], D.Verkindt[1], F.Vetrano[3], A.Viceré[3], J.-Y.Vinet[6], H.Vocca[9], M.Yvert[1]

[1]Laboratoire d'Annecy-le-Vieux de Physique des Particules (LAPP), IN2P3/CNRS, Université de Savoie, Annecy-le-Vieux, France
[2]European Gravitational Observatory (EGO), Cascina (Pi) Italia
[3]INFN, Sezione di Firenze/Urbino, Sesto Fiorentino, and/or Università di Firenze, and/or Università di Urbino, Italia
[4]LMA, Villeurbanne, Lyon, France
[5]INFN, sezione di Napoli and/or Università di Napoli "Federico II" Complesso Universitario di Monte S.Angelo, Italia and/or Università di Salerno, Fisciano (Sa), Italia
[6]Departement Artemis - Observatoire Cote d'Azur, BP 42209, 06304 Nice , Cedex 4, France
[7]LAL, Univ Paris-Sud, IN2P3/CNRS, Orsay, France
[8]ESPCI, Paris, France
[9]INFN Sezione di Perugia and/or Università di Perugia, Perugia, Italia
[10]INFN, Sezione di Pisa and/or Università di Pisa, Pisa, Italia
[11]INFN, Sezione di Roma and/or Università "La Sapienza", Roma, Italia
[12]NIKHEF, NL-908 DB Amsterdam and/or Vrije Universiteit, NL-971 HV Amsterdam, The Netherlands
[13]INFN, Sezione di Roma Tor Vergata and/or Università di Roma Tor Vergata, Roma, Italia

Abstract. VIRGO, a French-Italian collaboration located in Cascina (Pisa, Italy) aiming at the detection of gravitational waves, is a ground based power recycled Michelson interferometer, which arms are 3-km-long Fabry-Perot suspended cavities. The VIRGO first scientific data taking has started in mid may 2007 in coincidence with the corresponding American detectors.

The optical scheme of the interferometer and the various optical techniques used in the experiment, like the laser source, control, alignment, stabilization and detection strategies are outlined.

corresponding author: Eric Genin, European Gravitational Observatory, Traversa H di via Macerata, 56021-Cascina, Italy. e-mail: eric.genin@ego-gw.it

The future upgrades that are planned for Virgo from the optical point of view, especially concerning the evolution of Virgo laser, are presented.
Finally, the next generation of gravitational wave detector (advanced VIRGO) is introduced from the point of view of the laser system.

1   Introduction

The Virgo detector is a Michelson interferometer with 3 km long Fabry-Perot cavities in its arms aiming at the detection of gravitational waves built by the French-Italian collaboration VIRGO [1]. This instrument is located near Pisa in Italy. Among all the ground-based detector, Virgo has been designed to have the best sensitivity in the low frequency region thanks to the particular seismic attenuators from which the mirrors are suspended. After the end of the construction (Summer 2003), and a very intensive commissioning phase, a first scientific data taking period has begun in May 2007 and should last for 4 months.

The apparatus is designed to achieve a relative displacement sensitivity of better than $\delta l/l = 10^{-21}/ \sqrt{Hz}$ between 20 Hz and 10 kHz. The sensitivity will be limited by seismic disturbances below 3 Hz, by thermal noise up to 100 Hz and by shot noise for higher frequencies.

In order to reach this extreme sensitivity, the Virgo detector uses special techniques to minimise the coupling of noise into the interferometric signal. The large optics (mirrors and beam splitters) are super-polished fused silica pieces with very low absorption and scattering (bulk absorption <1ppm/cm; coating absorption < 5ppm). They are located in an ultra-high vacuum system and suspended from a sophisticated seismic isolation system, the so-called superattenuator which offers a very high passive isolation [2]. However, the motion at the resonance frequencies of this system (between 10 mHz to 4 Hz) can be large and must be reduced by active control.

To guarantee a stable long-term operation and a high sensitivity the angular degrees of freedom have to be actively controlled.

In this article, the optical scheme of the interferometer, the laser system and the strategy of control are described.

The future evolution of Virgo in order to improve the detector sensitivity, mainly the laser system, is presented.

Finally, an introduction to the next generation of gravitational wave detector is given.

2   Principle of operation

Figure 1 shows a simplified optical layout of the VIRGO interferometer in the recycled configuration.
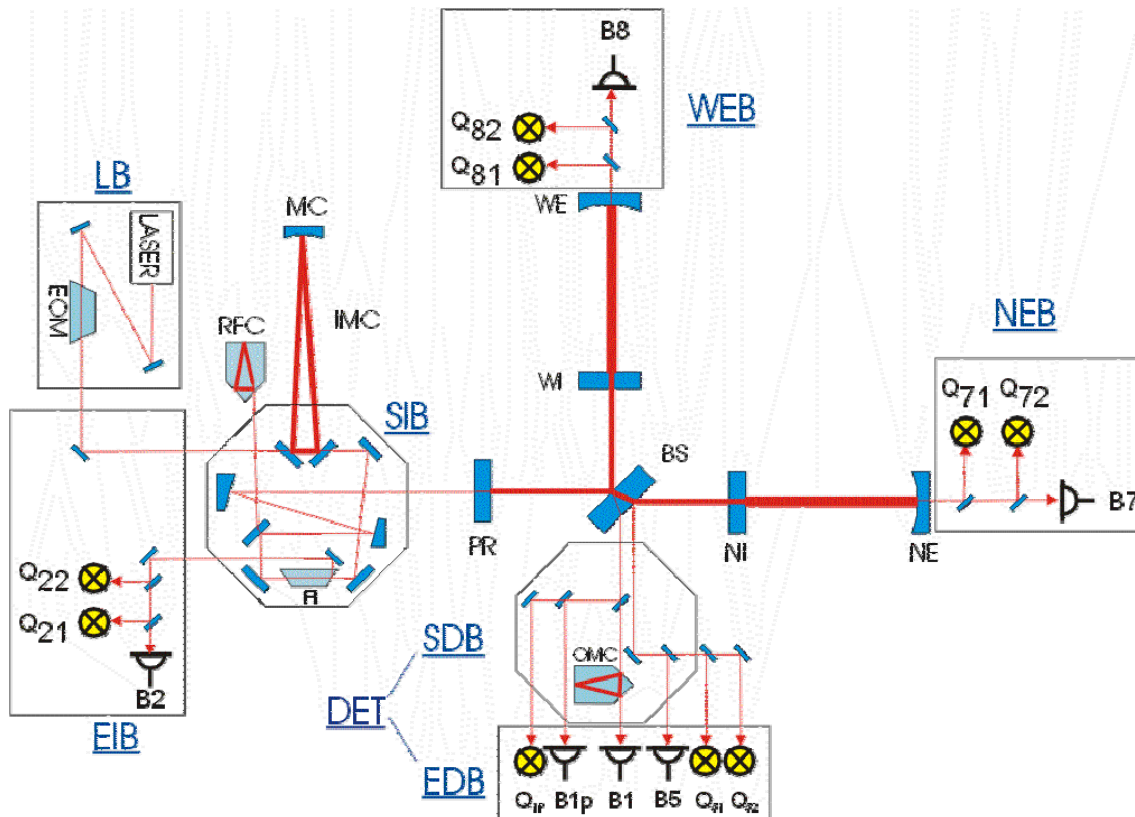
Fig.1 : Scheme of Virgo interferometer : The laser beam is directed on the *External Injection Bench* (EIB) into the first vacuum chamber, the injection tower, in which all optical components are attached to a suspended optical bench, the suspended *injection bench* (SIB). After passing the *input mode cleaner* (IMC), the beam is injected through the *power-recycling mirror* (PR) into the interferometer. The beam is split and enters the two 3 km long arm cavities, the *west arm* and *north arm*. The Michelson interferometer is held at the dark fringe so that most of the light power is reflected back to the *power-recycling mirror* (PR). In the final configuration the PR together with the Michelson Interferometer form a Fabry-Perot-like cavity in which the light power is enhanced. The light from the dark port of the beam splitter is filtered by an *output mode cleaner* (OMC) before being detected on a set of photodiodes (B1), which generate the main output signal of the detector. The other photodiodes shown in this schematic with names starting with **B** are used for longitudinal control of the interferometer; diodes named with a **Q** represent quadrants photo-detectors used for alignment control.

The laser light, 20W @1064nm provided by an injection locked master-slave solid state laser (Nd:YVO$_4$), enters the vacuum system at the *Suspended injection bench* (SIB). The beam is spatially filtered by a 144 m long input mode-cleaner cavity (IMC) before being injected into the main interferometer.

The laser frequency is pre-stabilised using the IMC cavity as a reference. The low-frequency stability is achieved by an additional control system that stabilizes the IMC length below 15 Hz to the length of a so-called reference cavity (RFC), a 30 cm-long rigid triangular cavity. Once the ITF is locked, the laser frequency stabilization loop (Second-Stage Frequency Stabilization : SSFS) is engaged in order to improve again the laser frequency stability by using the interferometer common mode.

A beam with 10W of power enters the Michelson interferometer through the power-recycling mirror.

It is split into two beams that are injected into the 3 km long arm cavities. The finesse of the arm cavities is approximately 50. The flat input mirrors and the spherical end

mirrors form a stable resonator with the beam waist being at the input mirrors with a radius of approximately 21 mm.

The interferometer is held on the dark fringe, and the expected gravitational wave signal will be measured in the beam from the dark port, which is passed through an *output mode cleaner* (OMC), which is a 2.5 cm long rigid cavity and then detected on photo diode B1 (in fact, B1 is a group of 3 photodiodes).

The interferometer control systems utilise the interferometer output signals and a modulation-demodulation method. For this purpose the laser beam is modulated in phase with a electrooptic modulator (EOM, see Figure 1) at f_{RF} = 6.26 MHz.

Such a phase modulation generates new frequency components with a frequency offset of $\pm f_{RF}$ to the frequency of the laser beam f_0. These frequency components are called *sidebands*, and the light field at f_0 is called *carrier*. The light detected by the photodiodes in several output ports of the interferometer are then demodulated with the same frequency f_{RF} or multiples of that frequency. The demodulated signals from single element diodes (B1 to B8) are used for the length control of the interferometer, whereas the demodulated signals from quadrant photodiodes (Q1p to Q82) provide control signals for the angular degrees of freedom of the interferometer mirrors.

The modulation-demodulation technique is commonly used in many interferometers, especially in the other interferometric gravitational wave detectors (LIGO (USA), TAMA (Japan) and GEO600 (GB and Germany) [3]–[5]). However, for each interferometer a unique control topology has been developed, depending on the details of the experimental realisation of the optical system.

Locking the cavities: Pound-Drever-Hall locking technique (PDH)

In order to keep the light resonating in the cavities formed by the suspended optics, their positions must be controlled within 10^{-13} m rms. To keep a cavity resonant ("locked"), the most intuitive way is to look at the transmitted/reflected power and keep it maximal/minimal. However, the dependence of the power on the length near the resonance is quadratic: the sensitivity is poor and, above all, the signal is symmetric on both sides of the resonance, so the servo cannot immediately tell which way to actuate.

With the PDH lock technique the light is modulated in phase using electrooptic crystals. A development to the first order in modulation depth shows that it produces two sidebands at frequencies $f_0 \pm f_{RF}$.

where f_0 is the frequency of the carrier and f_{RF} is the modulation frequency. This frequency is such that the sidebands are antiresonant in the 3km-long Fabry-Perot cavities. They are reflected by the front mirror, whereas the resonant carrier probes the end mirror. A fraction of the carrier is reflected by the cavity and interferes with the sidebands at the modulation frequency. If this signal is demodulated with the right phase, we obtain an error signal that crosses zero at resonance. This signal is an effective measure of the phase of the carrier leaving the cavity, it is therefore linear with deviation from resonance.

The PDH technique is used for Length Sensing and Control (LSC), but also for controlling angular motion by the Wavefront Sensing system as it is done for the alignment control of the suspended injection bench and suspended input mode-cleaner.

3   Virgo Injection system

The Virgo injection system consists of 4 main elements: the laser system, the beam monitoring system (reduction of beam jitter of the laser beam at low-frequency before the input mode-cleaner), the Input mode-cleaner (laser beam spatial and spectral filtering) and the suspended injection bench (under vacuum bench which enables to couple the light in the IMC and to match the laser beam on the interferometer by the mean of a parabolic telescope).

3.1   The laser source: an ultra-stable single mode high power laser

The Virgo laser source is a 20W continuous wave @1064nm provided by an injection locked master-slave solid state laser (Nd:YAG). The principle scheme of this laser is given in figure 2.
For the laser system which requires a very high powerful and stable laser, it has been chosen to injection-lock a high power monomode laser (slave laser) with a low power master oscillator.
The master laser is a commercial Innolight Mephisto 1000NE which is able to deliver a 1 W-continuous monomode laser beam with a FWHM lower than 1 kHz. The RIN is about -150 dB/Hz in noise eater mode.
The slave laser is a 20 W single transverse mode Neodymium-Vanadate (Nd:YVO4) ring laser (see figure 2) and has been developed by Laser Zentrum Hannover (LZH). The laser crystals are pumped longitudinally. The pump energy is delivered from fibre coupled laser diodes. Operated stand alone the laser oscillates in multiple longitudinal modes and emits parts of the power in two separated laser beams.
Injection locking is a well-known technique [7] to capture all the power of a multifrequency high power laser into a single frequency output without any loss of power. With this technique we can also transfer the frequency stability and the amplitude stability of the master laser to the slave laser.
2 mirrors of the slave are mounted on piezo-tranducers in order to allow to compensate for external acoustic and mechanical perturbations. In order to keep the slave laser in the locking range relative to the master laser frequency its length is controlled using the well known Pound-Drever-Hall (PDH) locking technique.
The phase of the master is modulated at 14 MHz using a $LiNbO_3$ phase modulator. Assuming that the carrier is close to the resonance of the slave laser cavity, the light reflected by the slave contains a 14 MHz beat note between the reflected non-resonant sidebands and the slave oscillation which is phase shifted from the master carrier by φ [8]. Then, the amplitude of the 14 MHz beat note is proportional to φ and the demodulation gives an error signal which is sent to the electronic servo system feeding the two piezo-transducers of the slave.

These piezo transducers allow to compensate for frequency shifts of the slave cavity. The first one yields a frequency correction sensitivity of 5MHz/V, a servo bandwidth from DC to several kHz, and a frequency shift up to 12 GHz. The second one (the fast one) yields a frequency correction sensitivity of 360 kHz/V, a bandwidth of 100 kHz and a frequency shift up to 10 MHz.

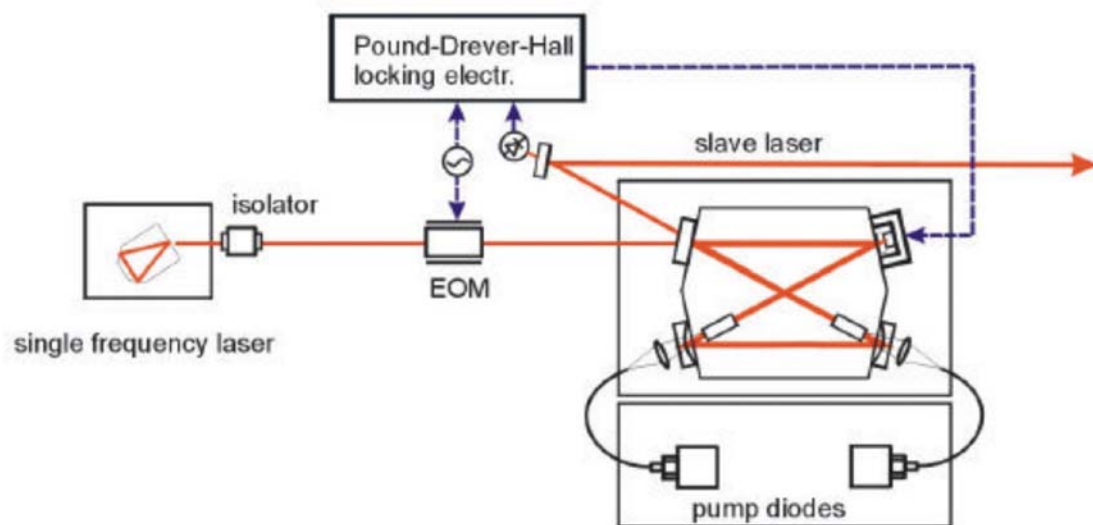The unity gain frequency (UGF) for the overall servo loop is 100 kHz.

Fig.2: Virgo Laser based on injection locking technique: The master is an Innolight NPRO laser (single frequency laser) and the slave laser contains 2 Nd:YAG rod pumped by fiber-coupled diodes.

The laser frequency is pre-stabilized using the IMC cavity as a reference. The low-frequency stability is achieved by an additional control system that stabilizes the IMC length below 15 Hz to the length of a so-called reference cavity (RFC) [9].

3.2   Beam Monitoring System (BMS), IMC and SIB automatic alignment.

In order to send the laser beam through the ITF, we use an in-vacuum suspended bench which has two scopes: to clean spectrally and spatially the laser beam by the mean of a suspended triangular cavity called the Input Mode-Cleaner (IMC) and to adapt the laser beam size to the interferometer to maximize the coupling efficiency. The beam monitoring system (BMS) is used to keep the laser beam in a fixed position before entering on the SIB and the Injection bench automatic alignment system to keep the IMC cavity locked and avoid a drift of the SIB.

3.2.1 Beam Monitoring System

Before entering the tower, we used 2 quadrant photodiodes (BMS_QN and BMS_QF) and 4 piezo actuators to keep the beam in a reference position (cf. figure 3). This system enables to lower the beam jitter at low-frequency and to keep the beam in a given reference position. The unity gain of the loop is around 1 Hz. It gives also a good monitor of the beam jitter noise before the Input Mode-Cleaner.
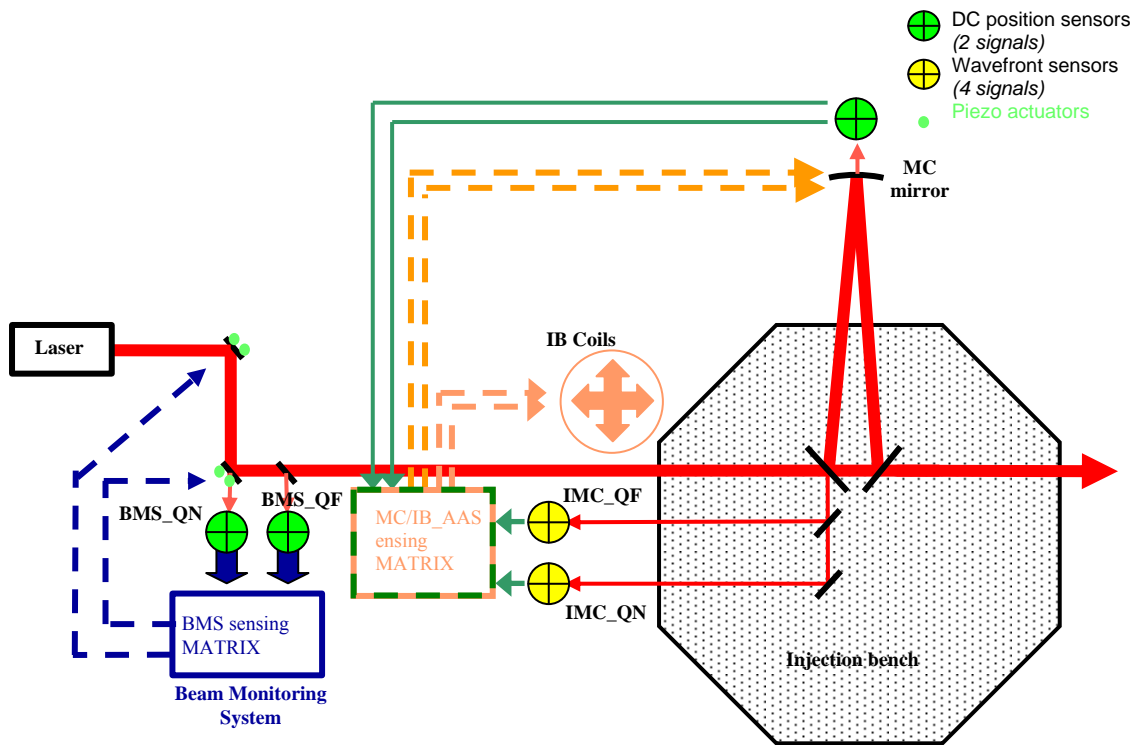
Fig.3: Beam Monitoring System and Injection system Automatic alignment: Piezo actuation is used for BMS corrections and Coils-magnet control is used to control the injection bench and IMC position.

3.2.2 Input Mode Cleaner

This is a 287 m (round trip length) long suspended triangular cavity, that aims to filter spatially the laser beam before entering in the ITF but it also improves the laser frequency and power fluctuations (triangular geometry has been chosen in order to avoid back-reflection of the light in the laser).

In order to couple the maximum of light in the ITF recycling cavity it is necessary to filter spatially the laser beam to have a TEM_{00} spatial distribution of this beam. In fact, beam distortions are created by the optical components (as electro-optical modulators) which are on the light path between the laser and the IMC.

The IMC behaves as a first order low-pass filter for the power and frequency fluctuations of the incoming laser beam. The fluctuation suppression factor is given by:

$$H(f) = \frac{1}{\sqrt{1 + \left(\dfrac{f}{f_0}\right)^2}} \qquad (1)$$

where f_0 is the IMC cavity pole ($f_0 = c/4LF$, L : cavity half round-trip, F : cavity finesse).

For L=143.5 m, f_0 = 508 Hz.

Amplitude and frequency fluctuations of the incoming beam are suppressed as $1/f$ above the cut-off frequency f_0.

Using the BMS quadrants to measure the beam jitter before the input mode-cleaner, we estimated that the angular beam motion was lower than 2.10^{-2} urad/$\sqrt{Hz}$ between 1 *Hz* and 10 *kHz*.

Because higher-order modes are suppressed by the input mode cleaner, beam jitter is decreased by a factor that is given by the following expression (assuming that the IMC is much more stable that the beam because it is suspended):

$$A_S = \sqrt{\frac{T_{mn}}{T_{00}}} = \sqrt{\frac{1}{1 + \left(\dfrac{2}{\pi} F \sin\left(\dfrac{2\pi\Delta\upsilon_{mn}}{c} L\right)\right)^2}} \qquad (2)$$

where A_S is the jitter amplitude attenuation factor; $\Delta\upsilon_{mn} = \dfrac{c}{2L}(m+n)\dfrac{1}{\pi}\arccos\sqrt{g}$ and $g = 1 - L/R_C$; R_C is the end mirror radius of curvature.

The filtering efficiency depends on the factor $\dfrac{2}{\pi} F \sin\left(\dfrac{2\pi\Delta\upsilon_{mn}}{c} L\right)$ has to be as high as possible for the lower-order modes in order to minimize the beam jitter.

To satisfy this condition F has to be as high as possible and the IMC has to be non-degenerated, i.e., $(m+n)\arccos\sqrt{g} \neq n\pi$ (n is an integer).

3.2.3 Injection bench and IMC automatic alignment

6 degrees of freedom (d.o.f) are controlled, 4 for the injection bench (θ_x, θ_y, θ_z and z) and 2 for the IMC (θ_x, θ_y).

IB and IMC d.o.f's are controlled with a mix of long lever arm DC controls using the position of the beam on a quadrant photodiode located below the IMC end mirror as you can see on figure 3, 4 interferometric signals (Ward signals: for a single Fabry-Perot cavity the alignment control signals can be derived in reflection of the cavity using Ward method [10]) through out 2 wavefront sensors (IMC_QN and IMC_QF on figure 3). The performances of this control are that all the angular degrees of freedom are controlled within ± 0.5 µrad with a unitary gain frequency (UGF) of several Hz for all the degrees of freedom except IB z that have a very low UGF.

4   Virgo Detection system

The light exiting the interferometer at the output port is optically filtered using an output modecleaner (OMC). The OMC is a short rigid triangular cavity made from a piece of silica properly polished and coated [11]. This cavity has an optical length of about 2.5 cm and a finesse of 50. Once filtered, the light is split over an array of 3 InGaAs photodiodes. These are 3 mm diameter photodiodes (specially developed by Hamamatsu) with quantum efficiency larger than 90%.

Their arrangement allows to easily adapt the number of used photodiodes to the dark fringe power (each photodiode can manage up to 100 mW). The current flowing in each photodiode is pre-amplified before being synchronously detected at the main modulation frequency (6.26 MHz). One percent of the dark fringe light is extracted before it enters the output mode-cleaner (B1p beam in Fig. 1) and detected to help the interferometer lock acquisition process. The light reflected by the second face of the beam splitter (B5 beam in Fig. 1) is also gathered and used for interferometer control purposes. Similar photodiodes detect the two beams transmitted through the two end mirrors (B7 and B8). Also placed at all these output ports are the quadrant photodiodes used for automatic alignment [12] purposes and the CCD cameras which are used to help the interferometer pre-alignment.

Once the interferometer is locked on the dark fringe, the output mode-cleaner length should be locked to the laser wavelength in order to have it resonant with the TEM00 mode. To achieve this, the output mode-cleaner optical length is varied by scanning its temperature and the transmitted beam is monitored by a digital CCD camera. The camera image is read by a realtime CPU that continuously compares the beam shape with the expected TEM00 mode. The image is processed 10 times per second and a χ^2 variable is calculated at this rate. As the χ^2 variable becomes smaller than a user defined threshold, the output mode-cleaner control system tries to lock it to the resonance. Typically the lock attempt is started when the transmitted power is about 15% of the power at the resonance. In order to get an error signal, the OMC length is modulated at 28 kHz using a piezoelectric actuator. The error signal is synchronously detected at this same frequency by demodulating the current flowing in the photodiode placed on the transmitted beam and is used to adjust the temperature of the cavity. This is achieved by means of a digital feedback also running at 10 Hz and having a unity gain around 20–30 mHz.

5   Current performances and mid-term evolution

The main performances of the apparatus are characterized by the sensitivity curve of the instrument (cf. Fig. 4). This sensitivity is limited by different sources of noise [13] depending on the bandwidth. At low frequencies (below 100Hz), the sensitivity is limited essentially by "control noises" (angular and longitudinal). In the middle frequency range (100-1000Hz), the limiting noises are environmental noises coupled by various sources of diffused light. Finally above 1kHz, the sensitivity is shot noise limited.
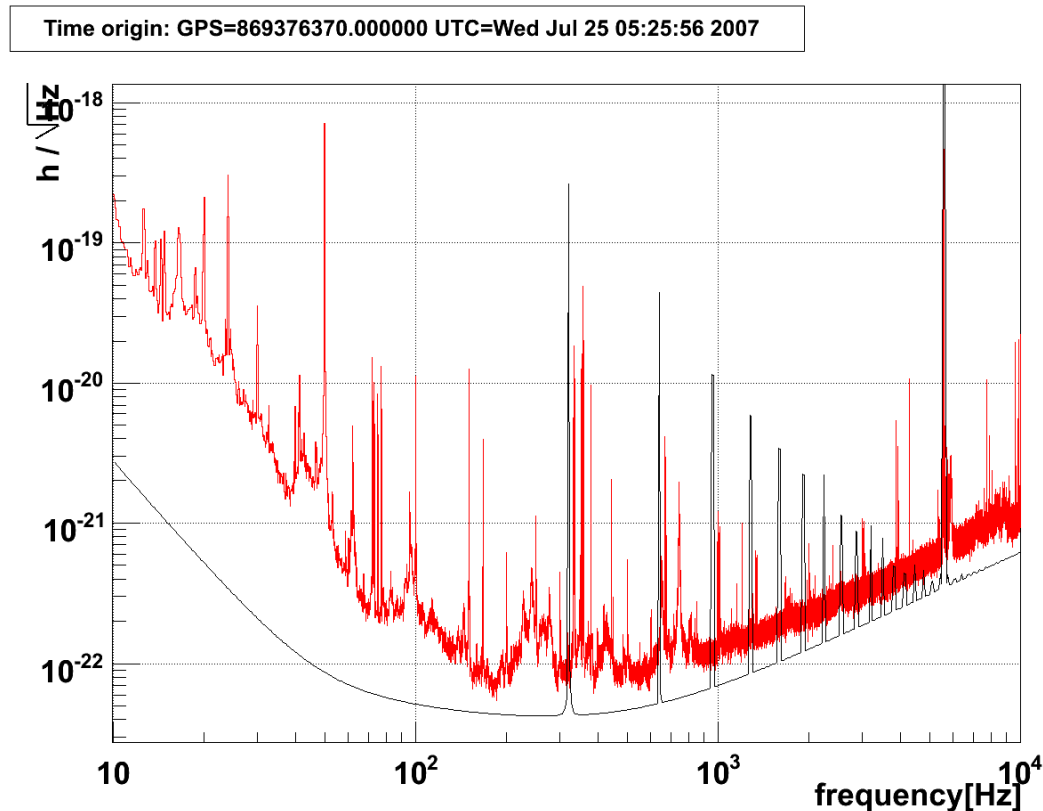

Fig. 4: Recent Virgo sensitivity curve (red curve) compared with Virgo design sensitivity (black curve).

Virgo is currently facing two major problems in term of sensitivity performances: diffused light related noises and input power limitation due to thermal lensing effects. Many activities have already started to overcome these limitations and will go on after the scientific run.
For what concerns the diffused light, we are fighting on 3 fronts: the transmission of the far end mirrors, the dark port and the reflection port of the interferometer. In each case,

some light from the main beam is backscattered and acts as a vector which couples the environmental noise (acoustic and seismic) to the interferometer output limiting the sensitivity in various spectral regions between 10 Hz and 1 kHz. The work of mitigation is being done trying to decrease the environmental noise sources and at the same time improving diffused light problems substituting some optics with bigger and better quality ones and dumping all spurious beams present at the different interferometer ports.

As a consequence of the thermal effects observed in Virgo [6], the interferometer is being run with 8 Watts at the input instead of the 10W that could be delivered at the output port of the Input Mode-Cleaner.

This has been shown to be an experimental limit. Beyond this limit, the resonance properties of the sidebands' fields (mandatory to build the Pound-Drever signals used to control the length of the cavities) in the recycling cavity is changed in such a way that the longitudinal control of the optical cavities becomes unstable.

The phenomenon can be explained as follows: the input mirrors of the Fabry Perot cavities are absorbing some energy (typically, 0.7 ppm/cm for the substrate and 1.2 ppm for the coating). As the temperature of the mirror is changed in a non spatially uniform way, the optical index of the material is changed in a proportional way creating a virtual lens in the recycling flat-flat cavity.

The sidebands, which are resonating only in the recycling cavity (and not in the arms FP cavities as the carrier), are then degenerated in higher order modes whom resonance properties are different. As we are using the optics with the lowest absorption available right now, the only solution is to implement a thermal lensing compensation system. A concept based on the systems already running in equivalent experiments (LIGO, GEO) is currently being developed and should be integrated at the beginning of 2008. It consists on a CO_2 laser focalized on the mirror with a ring shape designed to uniformize the temperature in the substrate.

6   Virgo +: a first upgrade to Virgo.

6.1   Description

Before reaching a second generation of interferometers, to get a sensitivity enhanced by a factor 10 respect to the first generation, there is the possibility to perform minor upgrades, thus improving significantly the sensitivity of the detector. The list of these modifications have been gathered under the project name "Virgo+".

From the optical point of view, Virgo+ should improve the shot noise which is limiting the sensitivity at high frequency and also the middle frequency region by the mean of an increase of the ITF input power up to 30 Watts.

To obtain this goal, assuming a typical 60% transmission of the IMC, there is the need to amplify the 20 watts current laser source to 50 watts. This will be achieved through a

4 stages Nd:YVO$_4$ amplifier provided by Laser Zentrum Hannover. This amplifier is currently under test. A power of 64W at the output port of the amplifier has been shown on a test bench. In this configuration it has been demonstrated that we can have more than 50 watts power at the output port of the Pre Mode-Cleaner.

The Pre Mode-Cleaner cavity, a triangular 13 cm half round trip long cavity (finesse=500) made of Zerodur and installed in a vacuum tank, will be devoted to filter out the amplitude fluctuations of the laser. The principle scheme of Virgo+ laser system is given in figure 5.
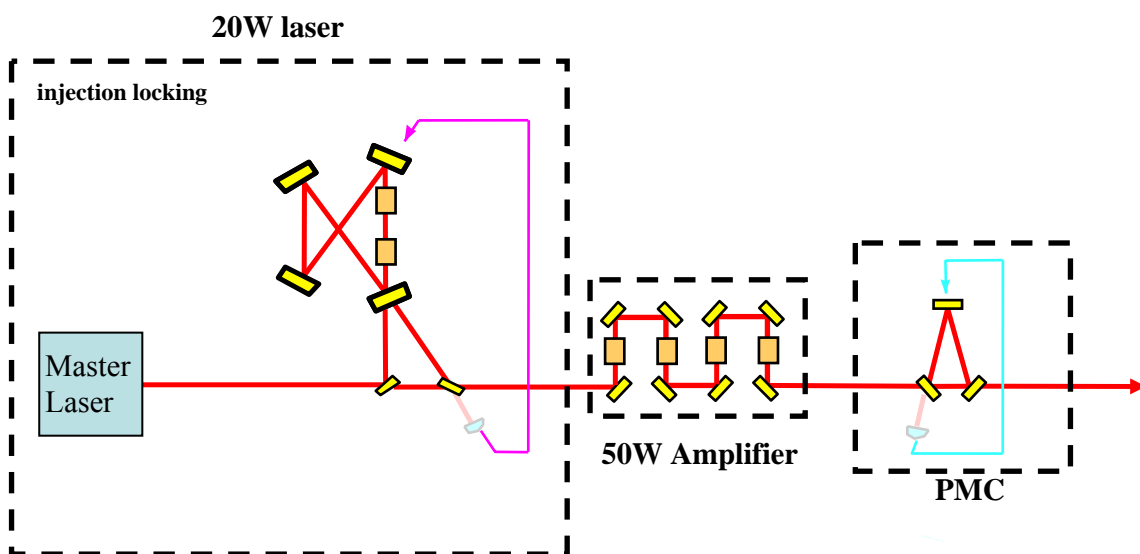

Fig.5: Power enhancement of Virgo laser: Virgo 20 watt injection-locked laser amplified by a 4 stages amplifier with a Pre Mode Cleaner (PMC).

Finally, an improvement of sensitivity will be obtained by enhancing the power stored in the interferometer by increasing the finesse of the Fabry Perot cavities up to 150 (current finesse is 50).

These changes will probably induce some strong thermal effects in the Faraday isolator (located on the suspended injection bench) and also at the level of the input mirrors of the 3km Fabry-Perot cavities. Concerning the Faraday, we are currently studying the possibility to passively compensate for thermal lensing by adding a small piece of crystal in which the thermal lensing effect is contrary to the one experienced by the TGG crystal (magnetooptic crystal used in the Faraday isolator).

For the thermal lensing in the long cavities input mirrors, as previously explained it consists in projecting a CO_2 light ring on the input mirrors to uniformize the temperature in the substrate and on the coating.

6.2   Noise budget and performances of Virgo +

With Virgo+ upgrade the sensitivity could be increased by a factor 2 to 4 with respect to Virgo design, depending on the frequency region (see figure 6). The commissioning

phase for Virgo+ should start in 2008 and end in 2009 to start a science data taking period in parallel with the equivalent American detector LIGO.
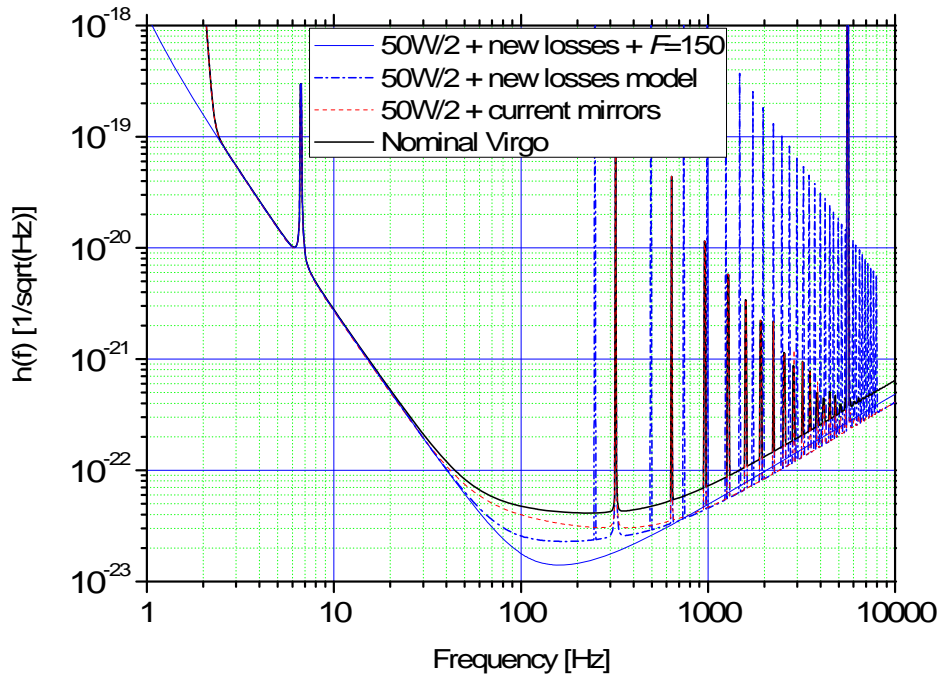

Figure 6: Virgo+ design sensitivity (considering that we have 25W entering in the ITF) for a Fabry-Perot finesse of 50 with current Virgo mirrors (red curve), with new low-losses mirrors (dash-dot bleu line) and with new low-losses mirror and a finesse of 150 (blue line). The black curve is the Virgo design sensitivity.

The figures of merit which are used for coalescing binaries sources (2 kinds of coalescing binaries signals are considered: a pair of neutron stars of 1.4 solar mass each and a pair of 10 solar masses binary black holes) [14] are the following :

First, the *Sight Distance@SNR=8*, it is the maximum distance at which an optimally oriented source would be detected with Signal to noise ratio (SNR) = 8.

Then, the *Events/Year@SNR=7* is the rate of events expected, assuming a conservative estimate of source density, and averaging over the geometrical parameters.

It is somewhat a nuisance that the two parameters refer to different SNR. The reason is that the theoretical estimates for the event rates are typically made using SNR=7, while other experiments (such as LIGO) use SNR = 8 for the sight distance.

With Virgo current sensitivity, we expect 1 event every 2000 years which is very low, this is why upgrades are necessary to develop gravitational waves astronomy.

D (MPc)	Event rate@SNR7 $yr-1$
10	3.44×10^{-3}
15	2×10^{-2}
20	3.00×10^{-2}
30	6.44×10^{-2}
40	1.21×10^{-1}
50	2.20×10^{-1}
70	7.08×10^{-1}
100	1.63
150	2.30
200	5.44
300	18.4

Table 1: Expected event rates at SNR = 7 as a function of the sight distance D (averaged over the source-detector relative orientation).

7   Advanced Virgo

Even if a first detection is possible, the sensitivity of Virgo and LIGO will not be sufficient to detect more than 0.1 event per year. For this reason it is important to prepare the upgrades of the present detector, considering that, for a uniform distribution of sources, an increase of the sensitivity by only a factor 2 will increase the expected event rate by about a factor 2^3 [12].

The first goal of Advanced Virgo is to enhance the sensitivity by a factor 10 respect to Virgo design sensitivity this should increase the rate of detectable event by a factor 1000.
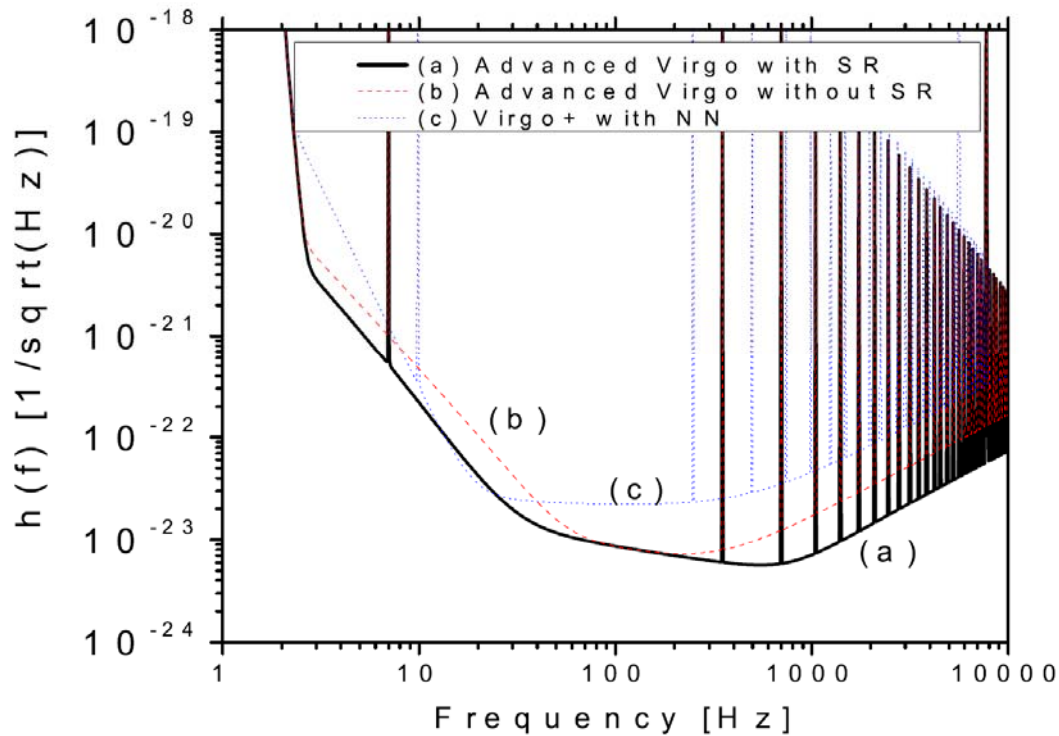
Figure 5: Preliminary Advanced Virgo noise budget assuming an input power of 100W, a mirror weight of 40kg, a recycling gain of 50 and a Fabry Perot finesse of 600.

The main upgrade of Advanced Virgo will be the increase of the input power up to 200W. Already, LZH is working on a 200W amplification module to be added in the optical path that could amplify a single-mode single frequency laser until 200 Watts with a multiple stage Nd:YVO$_4$ amplifier. There is also the possibility to recycle the signal using a signal recycling mirror (SR). As you can see on figure 5, with this configuration we should improve significantly the sensitivity of the detector between 3 and 50 *Hz* and above 300 *Hz*.

A so high power will induce some thermal lensing and birefringence problems on the optical components like polarizers, Faraday isolators, electrooptical modulators. In order to study these effects and compensate it, a research and development program has been put in place.

Within VIRGO collaboration, a huge effort is being done in order to implement an all fibered system on Advanced Virgo injection system. In particular, there is the possibility to replace the Input Mode Cleaner cavity with an optical fiber and to use an all-fibered laser as laser source providing a single-frequency 200 watts. This kind of laser has already been demonstrated experimentally [15].

Main issues deriving from higher power will be thermal effects. Side effects will concern the increase in scattering light.

8   Conclusion

Virgo giant power recycled Michelson interferometer has been presented mainly from the point of view of the different optical systems that are used in Virgo as the laser system, the injection system and the alignment control of the interferometer.
The current Virgo configuration needs to be upgraded in order to increase the probability of gravitational wave detection. The first step is the so-called Virgo + project which has for main goal to increase the laser power and the Fabry-Perot arm finesse up to 150 in order to improve the sensitivity of the detector between 100 Hz and 10 kHz by a factor 2. The second step, planned for the next decade, should improve Virgo sensitivity by a factor 10 and as consequence the rate of detectable event by a factor 1000. This should be the real starting point for gravitational wave astronomy.

9   Bibliography

[1] F.Acernese et al., The Virgo Interferometric gravitational Antenna, Optics and lasers in Engineering, 45, 478-487, (2007).
[2] S.Braccini et al., Measurement of the seismic attenuation performance of the Virgo superattenuator, Astroparticle Physics, 23, 557-565, (2005).
[3] D. Sigg *et al.*, "Commissioning of the LIGO detectors", *Class.Quant.Grav.*, 19(7), 1429–1435 (2002).
[4] M.Ando *et al.*, Current status of TAMA, *Class.Quant.Grav.* 19(7), 1409–1419,(2002).
[5] B. Willke *et al.*, The GEO 600 gravitational wave detector, *Class.Quant.Grav.*, 19(7), 1377–1387 (2002).
[6] M. Laval, Modeling of thermal effects in Virgo, Gravitational waves and experimental gravity, proceedings Rencontres de Moriond 2007 La Thuile, Italy (March 2007).
[7] A. E. Siegman, Lasers, University Science Books, 1986.
[8] R. Barillet, A. Brillet, R. Chiche, et al., An injection-locked ND:YAG laser for the interferometer detection of gravitational waves, VIRGO internal note, VIR-NOT-LAS-1390-010, 1996.
[9] Bondu *et al.*, Ultrahigh spectral purity laser for the Virgo experiment, *Optics letters*, vol. 21, No 8, 582–584 (1996).
[10] E. Morrison, B. .J. Meers, D. I. Robertson and H. Ward: "Automatic alignment of optical interferometers", *Appl. Opt.* **33** 5041–5049 (1994).
[11] R. Flaminio *et al.*, Interferometer signal detection system for Virgo experiment, Class. Quant. Grav. 19, 1857-1863 (2002).
[12] D. Babusci *et al.*, Alignment procedure for the VIRGO interferometer: experimental results from the Frascati prototype, Phys. Lett. A, 226, 31-34 (1997).
[13] E. Tournefier *et al.*, Noise budget and noise hunting in Virgo, Gravitational waves and experimental gravity, proceedings Rencontres de Moriond 2007 La Thuile, Italy (March 2007).

[14] R. Flaminio *et al.,* Advanced Virgo White Paper, VIR–NOT–DIR–1390–304, November 2005.

[15] Y. Jeong *et al.*, Single-frequency polarized ytterbium-doped fiber MOPA source with 264 W output power, Volume 2, 1065 – 1066, 16-21 May 2004.